Experimental study of wave loads on a small vehicle in close proximity to a large vessel

N. Xie*[1], G. Iglesias, M. Hann, R Pemberton, D. Greaves
School of Engineering, Plymouth University, Plymouth, UK

Abstract Operations involving the launch or recovery of a smaller vessel from a larger one are extremely dangerous in high sea states and, therefore, they are normally carried out in low to moderate sea states. However, this can be severely restrictive and in some situations, carrying out such operations in high sea states is unavoidable. Here we report on a detailed investigation of the interaction between two vessels of different size in order to characterise their hydrodynamic interaction under different conditions and to provide insight for operational purposes. Model experiments were conducted to investigate the hydrodynamic interaction between two vessels in close proximity in waves. Previous studies into this interaction have focused on two vessels with comparable size/displacement. This study focused on the interaction between vessels of very different sizes, a platform supply vessel and a lifeboat, at various separation distances between the two models and wave headings. It is found that the effect of the hydrodynamic interaction on the wave loads on the lifeboat model is substantial. The load responses show a strong non-linearity (high order harmonic components). In head waves, the effect of the hydrodynamic interaction on the wave loads is greater in the transverse modes (sway, roll and yaw) than in the longitudinal modes (surge, heave and pitch). The sheltering effects of the larger model on the lifeboat model were also evident from the experiments. The results of this investigation may be used to inform the planning of marine operations, such as the launch and recovery of a lifeboat or an Autonomous Underwater Vehicle (AUV) from a mothership and the transfer of equipment or personnel between vessels. The data will also provide a useful resource for validation of Computational Fluid Dynamics (CFD) codes and other numerical simulations, and can be used to better understand the limitations and potential widening of the operational weather windows and to ensure that operations are carried out safely.

Key words: model experiment; wave loads; hydrodynamic interaction; diffraction effect; radiation effect; launch and recovery

1 Introduction

The hydrodynamic interaction between floating bodies in close proximity is an important aspect for many marine operations involving two or more bodies, such as two vessels under replenishment at sea and loading/offloading between an FPSO and a tanker in an offshore oil field. There have been many experimental investigations of the hydrodynamic interaction of two vessels in close proximity in waves. Early studies on the subjects can be seen in the work of Oortmerssen [1], who conducted model experiments of hydrodynamic interaction between two bodies. Measurements were taken of the hydrodynamic interaction coefficients (added mass and damping coefficients) of a rectangular barge and a vertical cylinder for the radiation problem. During the experiments, each of the bodies was driven under a prescribed motion in calm water in turn, and resulting forces and moments on both bodies were measured. The length of the barge was close to the diameter of the cylinder. It was found that the greatest interaction effects occurred at high frequencies within the tested frequency range. When the two structures have the same size and similar motions amplitudes, it was found

* Corresponding author. E-mail address: nan.xie@plymouth.ac.uk (N. Xie)

that the hydrodynamic forces due to the motions of the neighbour can be of the same order of magnitude as the force induced by the body's own motions. McTaggart et al [2] carried out seakeeping experiments of semi-captive models of a supply vessel and a frigate in close proximity in a towing tank to study the effects of the hydrodynamic interactions on the (linear) wave forces/moments and motions. The results indicated that the presence of a larger vessel (supply vessel) can significantly influence the motions in waves of a smaller vessel (frigate), and the presence of the relatively smaller vessel has very little influence on the motion/loads of the larger vessel. Kashiwagi et al [3] conducted experiments in beam waves for the side by side arrangement of a Wigley hull model and a rectangular barge model. The lengths of the two models were the same. Added mass, damping coefficients of the Wigley hull, and the first order and steady drift wave forces/moments of the models were measured. Two separation distances were tested. It was found that the second order steady forces on each ship become large in both sway and heave. The sway steady forces on each ship are repulsive but the total force on both ships is positive; the heave steady forces on each ship are always positive in the vertical downward direction. Xu and Dong [4] conducted two sets of model experiments with two ship models arranged side by side in a towing tank. In the first set of experiments, wave exciting loads were measured when one model was fixed to a captive dynamometer and the other model was restrained in sway and yaw, while heave, roll, pitch motions were free, and surge amplitude was limited. The second experiment was designed to measure the free motions of the two partially-released ship models. The results indicated the significance of the hydrodynamic interaction on the transverse loads (sway, roll and yaw) and heave and roll motions but not so for pitch motions in head waves.

Hong et al [5] conducted numerical and model experimental studies for the interaction characteristics of side-by-side moored three vessels (FPSO, LNG and shuttle tanker). Global and local motion responses and drift forces of the three vessels are compared with those of calculations. Helmholtz resonance phenomena were captured from the measured relative wave at mid ship of FPSO to which LNG side-by-side moored. It was found that the strength of interaction is reduced as heading angle changes from beam sea to head sea and the biggest discrepancy is observed at head sea condition comparing to numerical predictions. Peng et al [6] conducted model experiments with two identical simplified FPSO models in a towing tank to investigate motions and free surface elevations between the two models, and found that the resonant wave elevation between the two ships decreases as the gap width increases. Huang et al [7] carried out wave tank model test investigations on the dynamic gangway response between monohull flotel and FPSO in non-parallel side-by-side configuration. The numerical calculations for the vessel motions, gangway relative motions were carried out by software HydroSTAR [8] and were compared with the model experimental measurements. It was found that the interaction triggers two types of couplings: coupling between two vessels as well as coupling within one vessel such as sway and pitch which does not exist in the single-body case. The results indicated that, by comparing single-body to multi-body cases, flotel's wave force and hydrodynamic coefficient become obvious fluctuating during short period range around 5-12s where strong hydrodynamic interaction happens in the multi-body case. Spikes were observed in flotel's motion while FPSO's doesn't change compared to the single-body case; It is also found that when flotel encounters beam sea in multi-body case, notable pitch motion is induced, which is considered negligible in single-body case. The relative

motion between the gangway point of flotel and landing point of FPSO possesses several peak periods and dynamic motion can be excited by waves in wide period range.

More recently, resonance of wave surface motion in the gap between two vessels (typically FPSO and FLNG) has attracted much interest in the hydrodynamics research community [9 10,11,12,13,14,15]. Peric and Swan [10] carried out experimental investigations of gap response between a ship-shaped vessel and a bottom-mounted box. Tests were conducted with a fixed and floating ship, and for regular, irregular and focused incident waves. Several different mode shapes were identified experimentally, as well as contributions from higher harmonics. Zhao et al [11] experimentally investigated the first and higher harmonic components of the gap resonant between two identical fixed rectangular boxes. The gap response was excited by transient wave groups (NewWaves). It was shown that for an incident group with appropriate frequency content, the linear gap response may be substantially smaller than the second harmonic component, which is strongly driven by quadratic coupling of the linear terms from the incident waves and occurs in the gap resonant modes. Sun et al [12] studied numerically free surface motions in the narrow gap between two vessels moored side-by-side by first and second order wave diffraction analysis. Additional peak frequencies were found in both linear and second order responses of the wave elevation in the gap. Pessoa et al [13] carried out numerical study of the coupled first order relative motions and the loads on the mooring lines and fenders (RAOs) of the side-by-side LNG floating system by software WAMIT [14] and compared the results with those of model experimental measurements conducted by Hansen et al [15]. The numerical calculations in head harmonic waves show a large hydrodynamic interface between the two ships, which induces motions in all degrees of freedom. There are resonant motions of the free surface between the two hulls. It is demonstrated that they are associated with the natural modes of the free surface in the gap and that these effects induce large relative motions. In general, the numerical method predicts well the measured responses (motions, relative motions and tensions in the moorings), however, there is a tendency to overestimate the yaw motion, and to a lesser degree the sway motions as well. Zhao et al [16] estimated gap resonance relevant to side-by-side offloading by using potential flow based software WADAM [17], HydroSTAR [8] and WAVELOAD-FD [18]. Model experiment was conducted to calibrate the artificial damping coefficient for the codes. The predicted RAO of the free surface elevations in the gap with corrected artificial damping agree well with experimental. Watai et al [19] conducted model experiments with a ship-like body and a box to investigate the gap flow for validation of a time-domain simulation method. The barge model was fixed while the vessel was restrained to have surge, heave and pitch motions only. The results shown that the gap resonant frequencies were lower for system with the largest gap width, different resonant frequencies have been observed for heave and pitch motions. The heave motions are significantly amplified due to the presence of a piston-type mode inside the gap, whereas the pitch motion is influenced by the occurrence of a second longitudinal mode. Ning et al [20] investigated numerically and experimentally the wave response at the gap between two barges of different draughts. The model test data were used to calibrate the artificial viscous coefficient of potential flow solver. It was found that the artificial viscous coefficient is determined not only by the relative barge draught but also by the propagating direction of the incident waves. The wave frequency corresponding to the largest wave amplitude at the gap is found to decrease, as either barge draught grows. The above

studies are mainly focused on the wave surface elevations in the gap and motions of the vessels involved, no detailed wave loading was reported

Watai et al [21] carried out wave tank model tests with two identical truncated circular cylinders, one was fixed and the other was imposed prescribed horizontal oscillatory motions with frequencies different from those of the incident waves. Measurements were made for the wave loads on the fixed body with a six DOF load cell. The tests were designed to provide validation data for numerical simulation concerning hydrodynamic interaction on bodies undergoing large relative displacements in waves. The hydrodynamic interaction of the two bodies is evident in the results. But only results of interaction for limited number of test cases were reported.

In the above studies for the hydrodynamic interaction, the two vessel/structures were of comparable size and displacement. For the hydrodynamic interaction between a large offshore structure/vessel and a relatively small body, a number of studies have been carried out for drifting and impact of a smaller iceberg near a large offshore structure (for example, Isaacson and McTaggart [22], Lever et al [23]). Gagnon [24] conducted comprehensive model tests to investigate hydrodynamic interaction between a floating ice mass and a tanker passing at speed. Sayeed et al [25] conducted experiments to measure wave loads on spherical masses (representing icebergs) at different proximities to and in front of a fixed structure (vertical cylinder). The experimental results showed that, as the body is positioned closer to the structure, the non-dimensional root-mean-square forces in the horizontal direction decrease, and the non-dimensional root-mean-square forces in the vertical direction increase. This study indicated that the radiation/proximity effect can be significant. The shapes of the bodies in the above experiments were relatively simple (sphere, cylinder).

Launch and recovery of small vehicles from a large vessel is a common operation in maritime sectors, such as with unmanned underwater vehicles from a patrol or research vessel, or lifeboats from offshore platforms or ships. The launch and recovery operations are potentially hazardous and remain challenging in higher sea states. To widen the operational weather window, advanced numerical modelling to simulate the motions and loads during the process is required to assist the planning and guide the operations at sea. A number of commercial software have the capability of predicting wave loads for the hydrodynamic interaction of multi-body problem, including first and second order loads [8,14,26,27]. While there are some experimental validations for the second order wave loads for single body case, for example [28], the validations for the higher order wave loads with hydrodynamic interaction of two bodies with very different size are less exposed. Furthermore, due to the complex nature of the interaction flow involving the mothership and the small vehicle, approach coupled RANSE/non-linear potential flow solvers and zone based method was proposed, this leads to a model experimental campaign to study the hydrodynamic interaction between vessels of very different size in close proximity and to provide validation data for the numerical simulation. To the authors' knowledge, experimental investigations for the hydrodynamic interaction between a small vehicle and a much larger vessel in close proximity are scarce. However, the complex hydrodynamic interaction between a lifeboat or AUV and the mothership are relevant, which demands an accurate estimation of loads and motions for the design of the deployment/recovery systems, control of vessel motion and trajectory, and operational procedures and selection of safe operating weather windows.

For the hydrodynamic interaction between a large vessel and a much smaller vehicle in close proximity, the influence of the small vehicle on the larger vessel will be limited, and the main hydrodynamic interaction will be the effect of the larger vessel on the smaller vehicle. The present paper describes physical model experiments of the hydrodynamic interactions between a small vehicle (lifeboat) and a large vessel (Platform Supply Vessel, PSV) in waves. Attention has been focused on the wave loads on the lifeboat model when it was fixed and in close proximity to the large (PSV) model. The PSV model was either fixed or partially released and was positioned side by side with the lifeboat model. The experiments investigated the influence of the separation distances between the two models and wave heading on the resulting wave loads. The experimental set-up and program is presented in section 2. Section 3 presents the test results and discusses the characteristics of the wave loads, effect of the separation distance and wave headings. Finally, conclusions are drawn in section 4.

2 Experimental Programme

2.1 Facilities

The model experiments were carried out in the Ocean Basin and a wave flume of the COAST Laboratory at the University of Plymouth. Length, width and depth of the Ocean Basin are 35m, 15.5m and 3 m, respectively. Waves are generated by 24 individually controlled hinged flap absorbing paddles. A convex absorbing beach was installed at the opposite end of the basin. The wave flume has length of 35m, width of 0.60m and water depth of 0.75m. The flume was equipped with a piston type wave-maker with active absorption capabilities and a foam beach at the opposite end.

Three groups of experiments were conducted: first, both the lifeboat model and the PSV model were fixed in a wave basin; the second was also with the lifeboat model fixed in the wave basin, but the PSV model was floating and free to heave, pitch and roll, but surge, sway and yaw were restricted; the third group consisted of the lifeboat model tests in a wave flume. The flume tests were conducted for the hydrodynamic interaction with an assumption of the larger vessel having infinite length.

2.2 Models and Instrumentation

The models used for the experiments were a PSV and a lifeboat with scale ratio of 1:20. The main particulars of the models are listed in Table 1.

Table 1 Main particulars of the test models

Specifications	PSV	lifeboat
Length, L (m)	3.51	0.50
Beam, B (m)	0.90	0.149
Draft, T (m)	0.261	0.054
Displacement, Δ (kg)	621.8	1.36
CG above keel, $\overline{KG}$ (m)	0.372	0.054
Roll radius of gyration, k_{xx}/B	0.375	0.35

Pitch radius of gyration, k_{yy}/L	0.25	0.25
Yaw radius of gyration, k_{zz}/L	0.25	0.25

The lifeboat model was mounted stationary with a rigid vertical column during the experiments. A six-axis load cell at its CoG (centre of gravity) was used to measure the wave loading on the lifeboat model. The capacities of the load cell are 125N for Fx and Fy, and 250N for Fz; capacity of Mx, My and Mz are all 25 N.m. Accuracy of the load cell is $\pm 0.1\%$.

For test cases where both models were fixed, the PSV model was mounted on a rigid framework connecting the model to the gantry over the basin (Fig.1).

A motion-constraining rig was designed and constructed for the PSV partially-released test cases. This consisted of three vertical guide rails connecting the rigid framework using linear bearing blocks and attached to the PSV model via universal joints on the longitudinal central plane. With this motion constraining rig, the PSV model was free to heave, pitch and roll, but surge, sway and yaw were limited (Fig.2).

In the wave flume tests, the lifeboat model was fixed in place using a vertical column via the load cell at the CoG position. Fig.3 shows the lifeboat model test in the wave flume.

For tests in the Ocean Basin, the two models were positioned in parallel with both CoGs at the same longitudinal location. The separation distance, s, was defined as the distance between the sides of the two models; in the case of the wave flume experiments, the separation distance was defined as the distance between the side of the lifeboat model and the flume side wall (Fig.4).

Resistance-type wave probes were positioned at various locations to register the wave profiles. As part of a data quality check, before conducting the experiments, both the load cell and waves were calibrated. Besides the measurement of wave loads and profiles, motions were measured using optical tracking, videos were recorded during the experiments and digital still photographs taken.

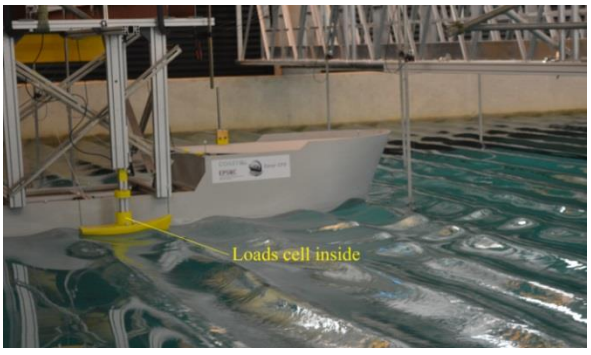

Fig. 1 PSV and lifeboat models both fixed in the wave basin

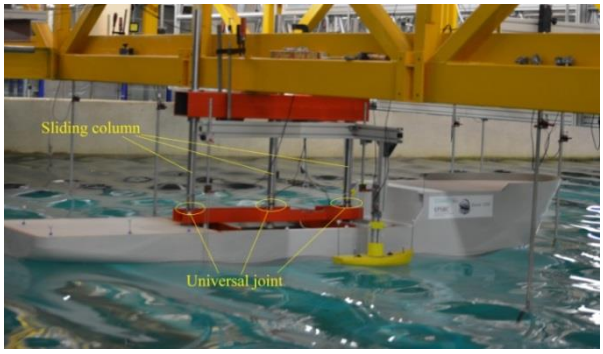

Fig.2 PSV model partially released in the wave basin

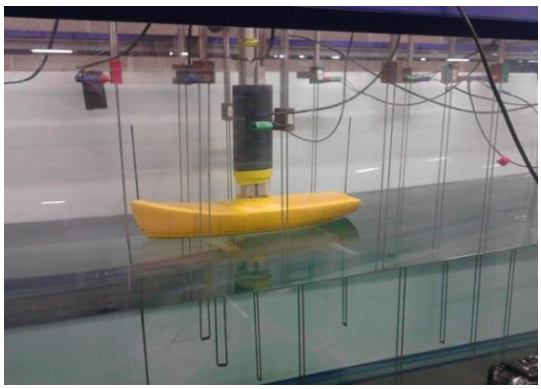

Fig.3 Lifeboat model in the wave flume

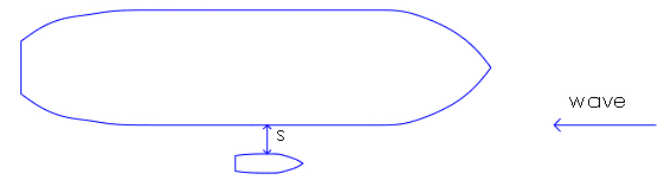

(a)

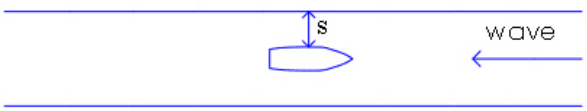

(b)

Fig.4 Models layout: (a) in the wave basin and (b) in the flume

2.3 Environment

The model experiments were carried out in regular waves. For the wave basin experiments, the wave periods were between 0.5 – 3.0 s, the wave amplitudes were 1% of the wave length and the maximum wave amplitude was 10 cm for the PSV model during the fixed tests; and 3.55 cm for PSV model during partially released tests. For the experiments in the flume, the wave periods were 0.5 – 1.5 s. The heading conventions were: 180^0 refers to waves coming from the bow (head waves); 90^0 refers to waves coming from port side (beam waves) and 0^0 refers to waves coming from the stern (following waves).

2.4 Methodology

Before carrying out the experiments, the PSV model was calibrated to the required weight, CoG position and the moments of inertia. The lifeboat model was mounted at the required waterline level. Experiments were carried out for the lifeboat alone, and at different wave headings and separation distances from the PSV model.

3 Model Experimental Results and Discussion

Observation during the model experiments shows the gap resonance doesn't exist because the gap length is typically about 10m while it is over 100m for FLNG offloading [10][11]. The data measured included time series of the 6-components of wave loads on the lifeboat model, motions of the PSV model and wave profiles from the wave probes. The surge force, F_x, is considered positive toward the bow of the lifeboat model, the sway force, F_y, is positive to the port side and the heave force, F_z, is positive upward. In analysing the data, time series of the raw data were selected after initial transient values had passed. Any static offset was removed to yield oscillating wave loads only. Low-pass filtering was applied to the recorded load signals to filter out high frequency noise and obtain the raw data of the wave loads.

3.1 Characteristics of the wave loads

In this section, we will explore the characteristics of the measured data for the wave load. Fig.5 shows an example of the harmonic analysis for the measured load cell data for sway force on the lifeboat model. The PSV model was fixed with separation distance to the lifeboat model, $s = 0.45L$ (where L is length of the lifeboat model) and in head waves (180^0). Wave amplitude and period are $\varsigma_a = 1.6cm$ and $T = 1\ s$, respectively. Fig. 5a is the time trace of the sway force for the raw data after low pass filtering to remove the high frequency noise and Fig. 5b is the spectrum of this raw data. The sway force amplitudes at the base frequency (1Hz, frequency of the incident wave), double frequency (2Hz) and triple frequency (3Hz) are shown. In terms of magnitude, the second and third harmonics are substantial when compared with the first harmonic force amplitude. Fig. 5c ~ 5e are the time traces of the first 3 harmonics of the sway forces, which can also be seen to exhibit different phases, and Fig. 5f shows the time history of the sum of the first 3 harmonics. The presence of significant higher order components indicates that the sway force of the lifeboat model due to the hydrodynamic interaction is non-linear. Fig.6 is the pitch moment of the lifeboat model for the same test case. In contrast with the sway force, the amplitudes of the 2nd order components

of the pitch moment are much smaller than those of the 1st order component and there is no 3rd order component.

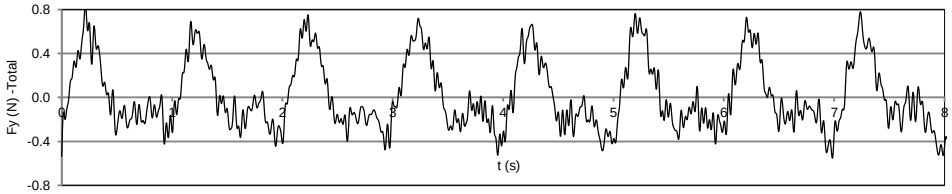

(a)

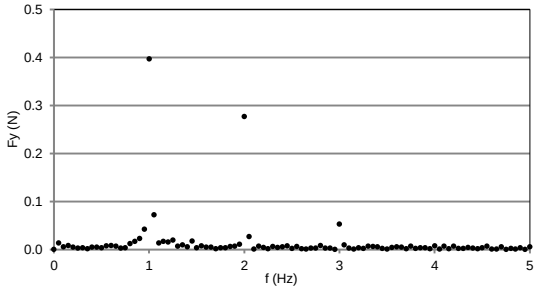

(b)

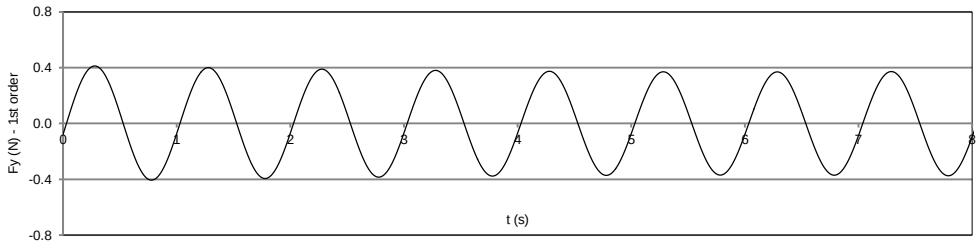

(c)

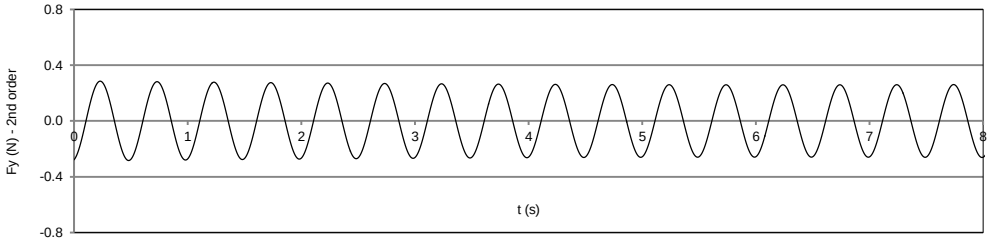

(d)

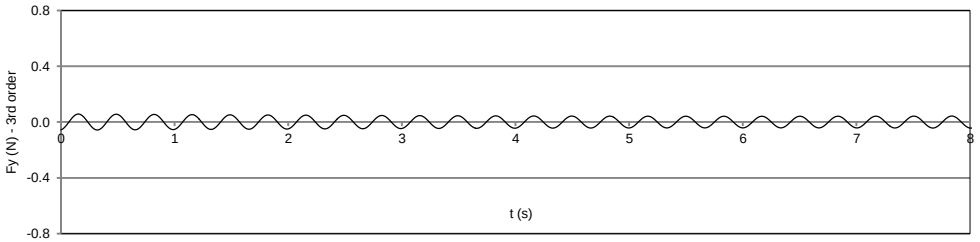

(e)

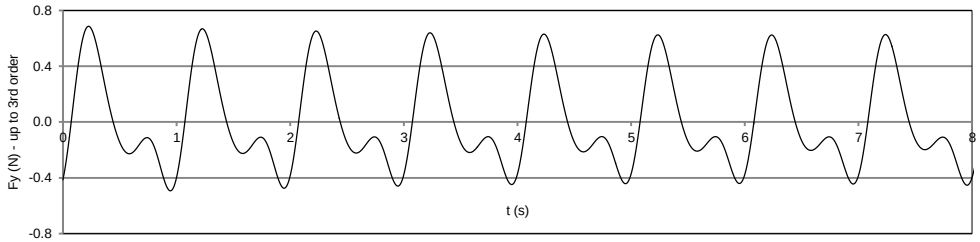

(f)

Fig.5 Time trace of sway force for the first 3 harmonics (wave period $T = 1s$, wave amplitude $\varsigma_a = 1.6cm$, PSV model fixed, 180^0, separation gap $s = 0.45L$), (a) raw data, (b) spectrum of raw data, (c) 1st harmonic time history, (d) 2nd harmonic time history, (e) 3rd harmonic time history, (f) combined sum of first three harmonics.

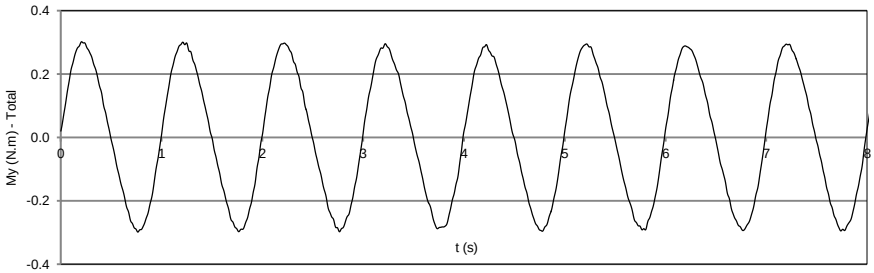

(a)

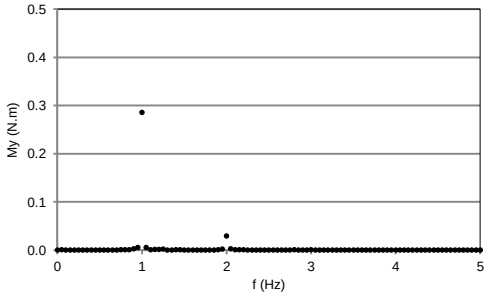

(b)

Fig.6 Time trace of pitch moment (wave period $T = 1s$,wave amplitude $\varsigma_a = 1.6cm$, PSV model fixed, 180^0, separation gap $s = 0.45L$), (a) raw data, (b) spectrum of raw data

Figs. 7 and 8 show, respectively, the amplitudes of the 1st, 2nd and 3rd harmonics for sway and heave forces of the lifeboat model during tests with the two models at the separation distance $s = 0.30L$ and the PSV model partially released tests in head waves. The force amplitudes were non-dimensionalised by $\rho gLB\varsigma_a$, where ρ is the water density, g is the acceleration due to gravity, L and B are the length and beam of the lifeboat model, and ς_a is the amplitude of the incident waves. The wave frequency was non-dimensionalised by $\omega' = \omega\sqrt{L/g}$. For the sway force, the amplitudes of the second harmonic were significant when compared with those of the 1st harmonic; at some frequencies, even the amplitudes of the 3rd harmonics were substantial (Fig.7). It is also noted in

Fig.7 that the amplitude of the 2nd harmonic component is larger than that of the 1st harmonic component at the non-dimensional frequency $\omega' = 0.95$ for sway force. An examination of the PSV model motions indicates that the heave and pitch motions of the PSV model are close to their peak responses at this frequency, and that the radiated waves due to large PSV model motions and the reflection waves from the tank walls amplify the hydrodynamic interaction between the two models, and further increase the non-linearity of the sway force on the lifeboat model. For the heave force (Fig.8), the loads mainly consist of the first (linear) harmonic, except at the lower frequency (longer wave length) range, where there was certain amount of component of the 2nd harmonic. This non-linearity may be caused by the non-vertical wall sided hull of the lifeboat model and its relatively low free board and the higher amplitudes of the incident waves (proportion to the wave length) and diffraction/radiation waves. The 3rd harmonic components were negligible.

In general, the analysed experimental results of the wave loads on the lifeboat model due to the hydrodynamic interaction between the two models in close proximity show that, the characteristics of the wave loads are non-linear, and this non-linearity of the wave loads is stronger for the transverse modes (sway, roll and pitch) than for the longitudinal modes (surge, heave and pitch). Some of previous studies only reported the 1st order components [2,4] or mean 2nd order forces [3,5] , or double frequency wave force for single body [28]. Some commerical software are able to to predict up to 2nd order forces, but not higher [8,14,26,27] , the 3rd order component is still substential due to the interaction in Fig.7.

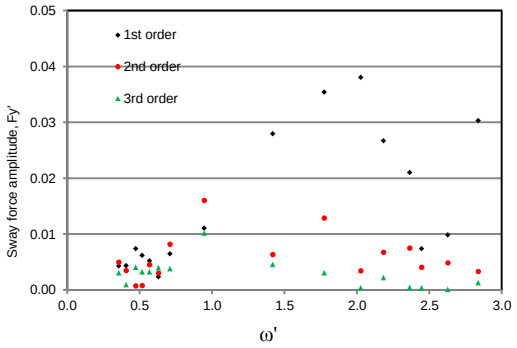

Fig.7 Non-dimensional amplitudes of sway force of the first 3 harmonics (PSV model partially released, 180^0, separation gap $s = 0.30L$)

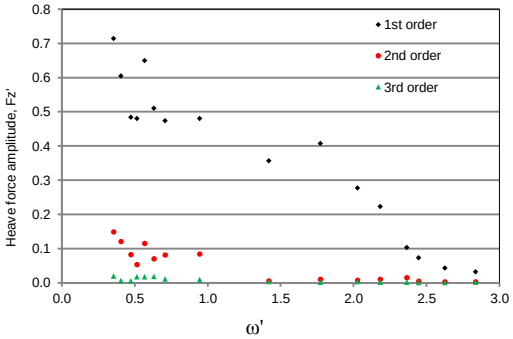

Fig.8 Non-dimensional amplitudes of heave force of the first 3 harmonics (PSV model partially released, 180^0, separation gap $s = 0.30L$)

3.2 Effect of separation distance

In this section, the effect of the separation distance between the models on the hydrodynamic wave loads on the lifeboat is discussed. The wave loads were shown in section 3.1 often to be non-linear in nature, and will therefore be represented using the RMS (Root-Mean-Square) of the signal. The load cell signals were filtered up to the third harmonic and the RMS was calculated for each component. The RMS of force and moment were non-dimensionalised by $\rho g B L \zeta_a$ and $\rho g B^2 L \zeta_a$, respectively.

As discussed in section 3.1, the longitudinal (surge, heave and pitch) wave loads show different characteristics from those of the transverse (sway, roll and yaw) wave loads, in the following sections, one longitudinal wave load and one transverse wave load will be selected for the discussions of the experimental results.

Figs. 9 and 10 show, respectively, non-dimensional RMS of sway and heave forces on the lifeboat model head waves (180^0) for 3 separation distances ($s = 0.45L, 0.30L$ and $0.15L$). The PSV model was fixed. The results of wave forces of the lifeboat only (no interaction) are also plotted. It is evident that there were influences of the hydrodynamic interaction between the two models on the wave loads of the lifeboat model when comparing with the lifeboat model only case. The wave loads in sway were more affected by the hydrodynamic influence than those for the heave force, in particular in the high frequency (short length) wave range in head waves. An uncertainty analysis (precision accuracy) following the ITTC recommended procedure [29] has been carried out for the wave loads, and examples of the analysis can be seen in the Appendix. In general, the accuracy of the measured longitudinal loads is higher than that of the transverse loads; overall, however, the uncertainty due to the precision accuracy does not alter the trends of the wave forces. In the lifeboat only case, the main wave field around the model consists of the incoming wave from the head direction and the diffraction wave of the lifeboat. Due to symmetry of the lifeboat hull geometry about its longitudinal symmetric plane, the dynamic pressure distributions due to both incoming and the diffraction wave fields are symmetric about this plane, and the transverse wave loads on the model negligible. The small sway forces on the lifeboat model in the low frequency range are believed to be due to some model misalignment during the model installation. It is observed that the trends of the effect of the separation distance on the sway force for the three tested gaps were less clear, and depend on the wave frequency. The effects of the separation distance on heave force were less obvious for the tested gaps and in comparison with the lifeboat model only case (Fig.10).

Figs. 11 and 12 show the non-dimensional RMS of pitch and yaw moments of the lifeboat model when the motions of the PSV model were partially released. The effect of the hydrodynamic interaction on the yaw moment is significant (Fig.12). Larger yaw moments were observed in the higher frequency range for the smallest separation gap ($s = 0.15L$). The influence of the separation gap on the pitch moment with the PSV model partially released is similar to that of the heave force in Fig. 10.

When the two models were in close proximity, the effects of the hydrodynamic interactions are greater for the transverse modes than for the longitudinal modes due to the changes of dynamic pressure field around the lifeboat hull.

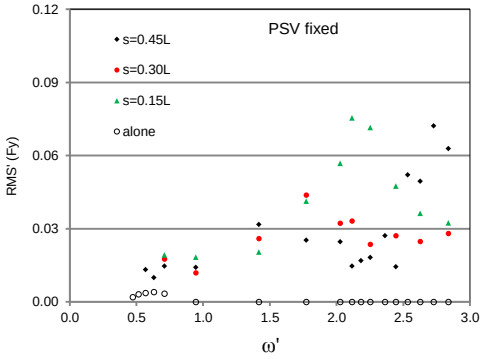

Fig. 9 Non-dimensional RMS for sway force at head waves (180^0, PSV model fixed)

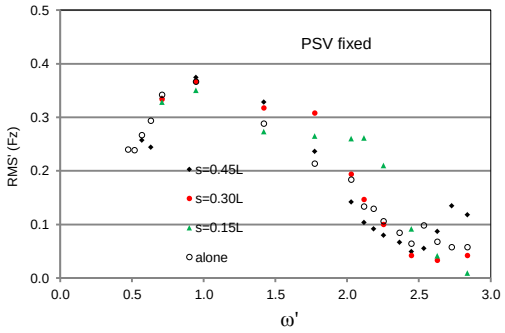

Fig. 10 Non-dimensional RMS for heave force at head waves (180^0, PSV model fixed)

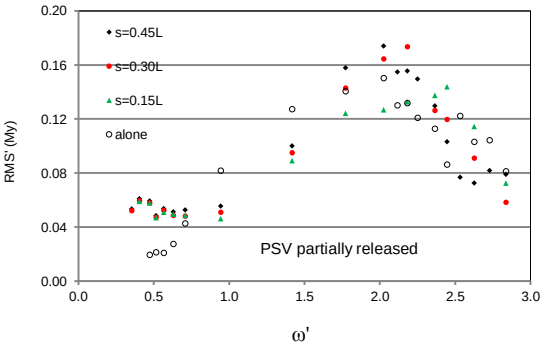

Fig. 11 Non-dimensional RMS for pitch moment at head waves (180^0, PSV model partially released)

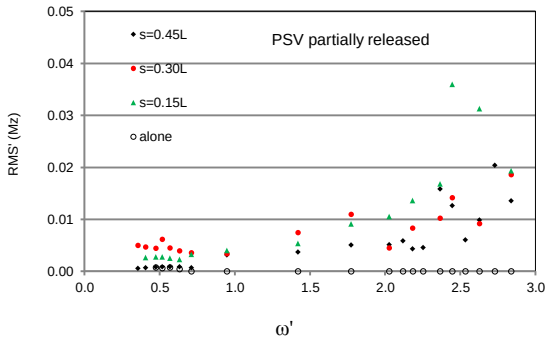

Fig. 12 Non-dimensional RMS for yaw moment at head waves (180^0, PSV model partially released)

It is worth to mention that the uncertainty analysis carried out in the Appendix is only part of the total uncertainty of the model experimental results: the precision accuracy. As for any wave tank model experiments, the tank wall interference is always a source of uncertainty. This is due to the limited tank width and there is no beach and the radiated waves propagate towards the tank side walls and cannot be damped, and will reflect back. To assess the effect of the tank wall for the present model experiments, wave records of a focused wave (NewWaves, [11, 30, 31]) test in head waves were analysed. Fig. 13 is the layout of the wave probes and the models in the tank. Two wave probes (P1 and P2) were located on the central plane of the wave tank and in front of the PSV model. The recorded wave elevations are shown in Figs. 14 and 15. The measured travelling speed of the focused wave pack is 1.7m/s, the second group of waves which is the reflection waves can be observed from Figs. 14 and 15. The travelling time is consistent with the distance between the probe locations and the side wall. The ratio between the minimum wave elevations of the second and the first group waves for wave probes P1 and P2 are 11.1% and 11.9%, respectively. This is the measure of the wall effect. It is worth to mention that the focused wave group contains many wave frequency components; the reflection ratio estimated above is a synthetic reflection coefficient. There will be different reflection coefficient for different wave frequencies. One can also notice that the magnitude of wave record of P2 is larger than that of P1, this is because wave probe P2 is located closer to the model than P1, and the measured wave of P2 includes more components from the diffraction waves. To assess the tank wall effect in more details, more works should be carried out and approach with combination of model experiments and suitable numerical simulations may be necessary.

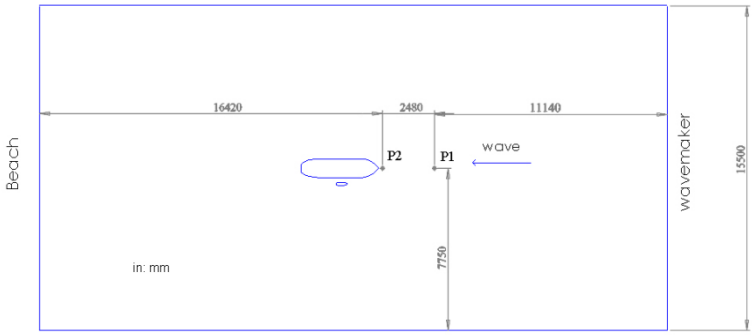

Fig. 13 Models and wave probes layout

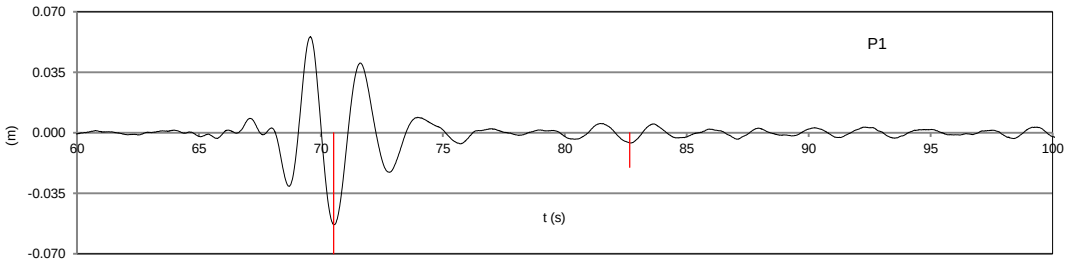

Fig. 14 Time history of wave elevation at probe P1

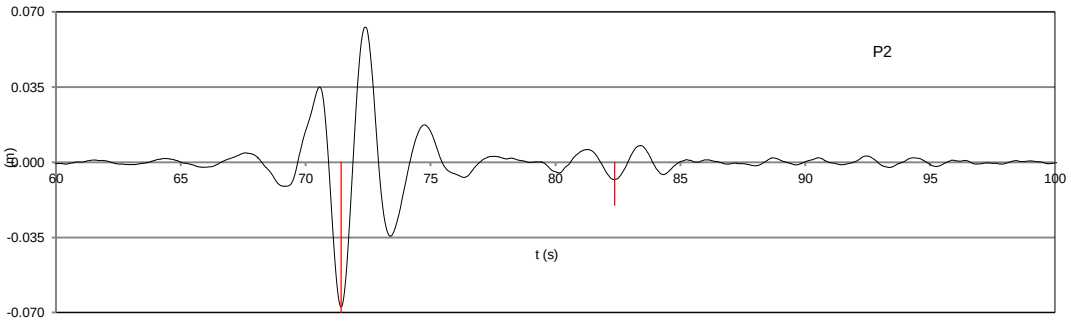

Fig. 15 Time history of wave elevation at probe P2

Figs. 16 and 17 show the sway force and pitch moment of the lifeboat model at the three separation distances ($s = 0.45L, 0.30L$ and $0.15L$) in the flume tests, in which $s = 0.45L$ corresponds to the model located at the central position of the flume. For sway force in Fig. 16, it is observed that, the closer the model to the flume wall, the higher is the sway force in general. There were two frequencies at which the interaction showed different behaviour. Further analysis indicates that these two wave frequencies correspond to wave lengths close to the 1st and 2nd modes of the cross resonance of the flume (wave lengths $\lambda = 0.6m$ and $1.2m$, respectively). The cross resonance frequencies also affect the pitch moment but to a lesser extent, see Fig. 17. At separation distance $s = 0.45L$, the lifeboat model was positioned at the central plane of the wave flume, and there was no sway force due to the symmetry.

It is also noted that the trends are less clear for the wave loads in the wave basin test than those in the flume in terms of non-dimensional wave frequency for the tested 3 separation distances. The reason is not clear yet, and needs further investigation.

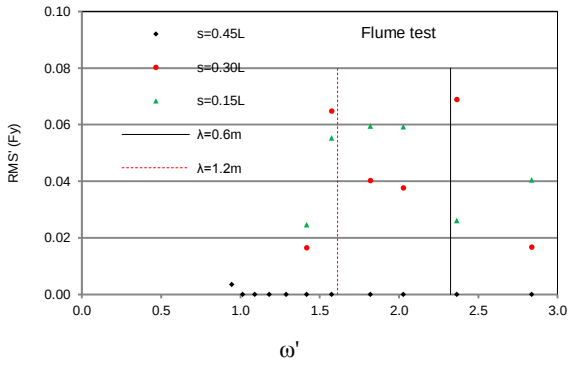

Fig. 16 Non-dimensional RMS for sway force (180^0, Flume test)

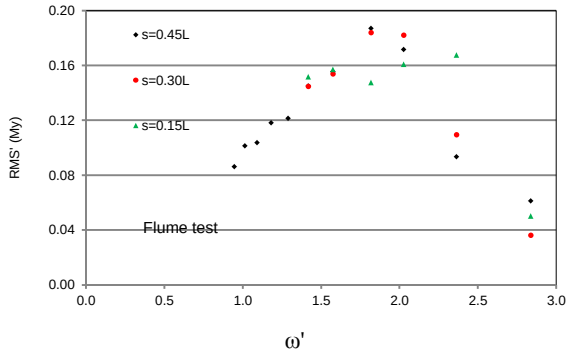

Fig. 17 Non-dimensional RMS for pitch moment (180^0, Flume test)

3.3 Effect of wave heading

Model experiments were carried out for the hydrodynamic interaction of the two models in various wave headings. The two models were positioned side by side in parallel with separation distance, $s = 0.45L$, and the lifeboat model at the starboard side of the PSV model. A wave heading of 210^0 corresponds to the lifeboat being at the windward side of the PSV model, while for wave headings of 165^0, 150^0 and 90^0, the lifeboat model was at the leeward side of the PSV model. Figs. 18 and 19 are the non-dimensional heave force and roll moment for test cases in which the PSV model was fixed. Figs.20 and 21 show pitch and yaw moments of the lifeboat model for test cases in which the PSV is partially released. The sheltering effect can be observed when comparing wave loads at 210^0 (lifeboat model at the windward side) and 150^0 (lifeboat model at the leeward side). The wave loads were considerably smaller for the lifeboat at the leeward side than those at the windward side. For the PSV partially released test cases, the pitch and yaw moments of the lifeboat model at the leeward side of the PSV model are also much lower than those at the windward side. The lifeboat model was exposed to the incoming waves and also to the diffraction/radiation waves of the PSV, while for the lifeboat model on the leeward side, the PSV model acts as a "shelter" and filters the incoming waves, producing a calmer wave field around the lifeboat model.

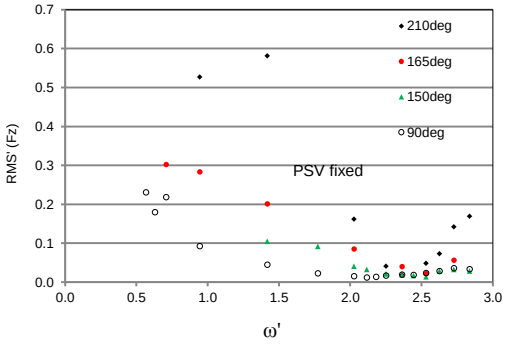

Fig. 18 Non-dimensional RMS for heave force at $s = 0.45L$ (PSV model fixed)

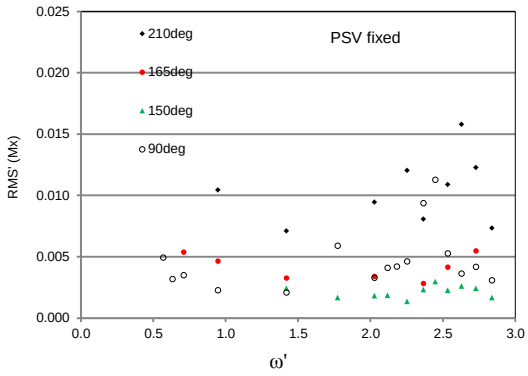

Fig. 19 Non-dimensional RMS for roll moment at $s = 0.45L$ (PSV model fixed)

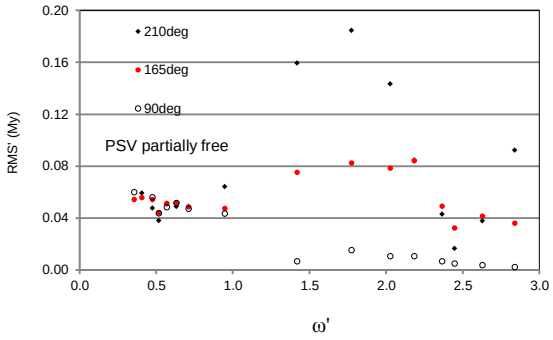

Fig. 20 Non-dimensional RMS pitch moment at $s = 0.45L$ (PSV model partially released)

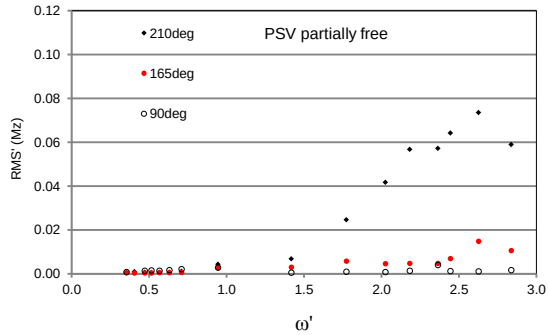

Fig. 21 Non-dimensional RMS yaw moment at $s = 0.45L$ (PSV model partially released)

4 Conclusions

Model experiments have been carried out to investigate the hydrodynamic interaction of two vessels in close proximity with a PSV model and a lifeboat model in waves. The experiments include tests in a wave basin and in a wave flume. The larger model was either stationary or partially released. Various separation distances between the models and wave headings were tested. The following conclusions may be drawn:

1. There are substantial effects of hydrodynamic interaction on the wave loads of the lifeboat model (smaller model) when it is in close proximity to the PSV model (larger model), and these need to be properly assessed when planning launch and recovery operations.
2. The transverse wave loads on the lifeboat model show strong non-linearity due to the hydrodynamic interaction, and therefore may not be predicted reliably by current design practice based on linear models and theory.
3. In head waves, the hydrodynamic interaction is stronger for the transverse loads (sway, roll and yaw) than for the longitudinal loads (surge, heave and pitch), and therefore detailed simulation of the transverse interactions will be necessary.
4. Positioning the lifeboat model at the leeward side of the PSV in waves will reduce its wave loads, in particular for shorter waves, although the sheltering effect is less pronounced in long waves.

The work of the present study may serve for validation of numerical predictions of ship/lifeboat hydrodynamic interaction due to the scarcity of appropriate experimental data. The results may be useful also for controlling vessel motions during such operations. Although the hydrodynamic interaction is evident, the trends in the influence of the separation distance between the two vessels on the wave loads are less clear, and will need further investigation. The non-linear effects and the hydrodynamic interactions seen may not be predicted by the current design practice based on linear numerical models and linear theory. To understand fully the likely response of a lifeboat or smaller vessel in operations close to a much larger vessel, simulations by experiments or fully nonlinear numerical model able to reproduce the nonlinear interactions properly is needed. This work provides important insight into the conditions under which launch and recovery operations may be carried out safely, and valuable validation data for models that can then be used for high fidelity simulation of such operations.

Acknowledgements

The authors would like to appreciate Sealion Shipping Limited for permission of use of the PSV vessel in the experiments and also be grateful for the support of Dr. K Monk and the COAST Laboratory during the experiments. The funding support from EPSRC through grant EP/N008847/1 is gratefully acknowledged.

References

[1] Oortmerssen, Van. G., 1979. Hydrodynamic interaction between two structures, floating in waves, Proceedings of second international conference on behaviours of offshore structures, pp. 339-356.

[2] McTaggart, K., Cumming, D., Hsiung, C. C., Lin, L., 2003. Seakeeping of two ships in close proximity, Ocean Engineering, 30, pp1051-1063.

[3] Kashiwagi, M., Endo, K., Yamaguchi, H., 2005. Wave drift forces and moments on two ships arranged side by side in waves, Ocean Engineering, 32, pp529-555.

[4] Xu, Y., Dong, W. C., 2013, Numerical study on wave loads and motions of two ships advancing in waves by using three-dimensional translating-pulsating source, Acta Mechanics Sinica, 29(4), pp494-502.

[5] Hong, S. Y., Kim, J. H., Cho, S. K., Choi, Y.R., Kim, Y.S., 2005. Numerical and experimental study on hydrodynamic interaction of side-by-side moored multiple vessels, Ocean Engineering, 32, pp783-801.

[6] Peng, H., M A Ali, M. A., Qiu, W., 2015. Hydrodynamic interaction of two bodies in waves, 30th IWWWFB, Bristol, UK.

[7] Huang, W., Li, B. B., Chen, X. B., Araujo, R., 2018. Numerical and experimental studies on dynamic gangway response between monohull flotel and FPSO in non-parallel side-by-side configuration, Ocean Engineering, 149, pp341-357.

[8] Chen, X. B., 2004, Hydrodynamics in offshore and naval applications, Proceedings of 6th International Conference on Hydrodynamics, Perth, Australia.

[9] Soares, C. G., Taylor, R. E., Ewans, K., 2015, Safe offloading from floating LNG platforms, Applied Ocean Research, 51, pp252-254.

[10] Peric, M., Swan, C., 2015, An experimental study of the wave excitation in the gap between two closely spaced bodies, with implications for LNG offloading, Applied Ocean Research, 51, pp320-330.

[11] Zhao, W. H., Wolgamot, H. A., Taylor, P. H., Taylor, R. E., 2017. Gap resonance and higher harmonics driven by focused transient wave groups, Journal of Fluid Mechanics, Vol.812, pp 905-939.

[12] Sun, L., Taylor, R. E., Taylor, P. H., 2015, Wave driven surface motion in the gap between a tanker and an FLNG barge, Applied Ocean Research, 51, pp331-349.

[13] Pessoa, J., Fonseca, N., Soares, C. G., 2015, Numerical study of the coupled motion responses in waves of side-by-side LNG floating systems, Applied Ocean Research, 51, pp350-366.

[14] Lee, C. H., 1995, WAMIT theory manual, Cambridge, MA, USA, MIT Press.

[15] Hansen, H. F., Carstensen, S., Christensen, E. D., Kirkegaard, J., 2009, Multi vessel interaction in shallow water, Proceedings of 28th OMAE, May 31-June 5, 2009, paper OMAE2009-79161.

[16] Zhao, W. H., Pan, Z. Y., Lin, F., Li, B. B., Taylor, P. H., Efthymiou, M., 2018, Estimation of gap resonance relevant to side-by-side offloading, Ocean Engineering, 153, pp1-9.

[17] SESAM User Manual – WADAM, 2016, Version 9.3, DNV GL, Hovik, Norway.

[18] Lloyd's Register, 2017, WAVELOAD-FD User Manual, Version 1.1 (Southampton, UK).

[19] Watai, R. A., Dinoi, P., Ruggeri, F., Souto-Iglesias, A., Simos, A. N., 2015, Rankine time-domain method with application to side-by-side gap flow modelling, Applied Ocean Research, 50, pp69-90.

[20] Ning, D. Z., Zhu, Y., Zhang, C. W., Zhao, M., 2018, Experimental and numerical study on wave response at the gap between two barges of different draughts, Applied Ocean Research, 77, pp14-25.

[21] Watai, R. A., Ruggeri, F., Simos, A. N., 2016, A new time domain Rankine panel method for simulations involving multiple bodies with large relative displacements, Applied Ocean Research, 59, pp93-114.

[22] Isaacson, M., McTaggart, K., 1990. Modelling of iceberg drift motions near a large offshore structure. Cold Reg. Sci. Technol. 19, pp47-58.

[23] Lever, J. H., Colbourne, B., Mak, L., 1990. Model study of wave-driven impact of bergy bits with a semi-submersible platform, J. Offshore Mech. Arct. Eng. 112 (4), pp313-322.

[24] Gagnon, R. E., 2004. Physical model experiments to assess the hydrodynamic interaction between floating glacial ice masses and a transiting tanker. J. Offshore Mech. Arct. Eng. 126 (4), pp297-309.

[25] Sayeed, T., Colbourne, B., Molyneux, D., Akinturk, A., 2017. Experimental and numerical investigation of wave forces on partially submerged bodies in close proximity to a fixed structure, Ocean Engineering, 132, pp70-91.

[26] AQWA Theory Manual., 2015, ANSYS, Inc. Canonsburg, PA, USA.

[27] DIFFRAC User Manual, 2012, MARIN, Wageningen, The Netherlands.

[28] Fonseca, N., Pessoa, J., Mavrakos, S., Boulluec, M. L, 2011. Experimental and numerical investigation of the slowly varying wave exciting drift forces on a restrained body in bi-chromatic waves, Ocean Engineering, 38, pp2000-2014.

[29] ITTC Recommended Procedures, 2002. Testing and extrapolation methods: Loads and responses, seakeeping, Seakeeping experiments, 7.5-02 07 – 02.1, Loads and Responses Committed of 23rd ITTC.

[30] Hann, M., Greaves, D., Raby, A., 2015. Snatch loading of a single taut moored floating waves energy converter to focused wave groups, Ocean Engineering, 96, pp258-271.

[31] Hann, M., Greaves, D., Raby, A., Howey, B., 2018. Use of constrained focused waves to measure extreme loading of a taut moored floating wave energy converter, Ocean Engineering, 148, pp33-42.

Appendix Uncertainty analysis

ITTC [29] have recommended procedures for loads and responses experiments and uncertainty analysis (2002). The precision accuracy analysis of the measured wave loads was performed in this study. Figs. A1 to A4 show examples of the precision limits for the wave loads. In general, the longitudinal wave loads (surge, heave and pitch) have a higher precision accuracy than the transverse loads (sway, roll and yaw).

One of the uncertainties is from the wave tank resonance. In the flume test cases, section 3.2 mentioned the effect of the first 2 resonance frequencies of the flume on the sway force. In the wave basin experiments, the first 2 resonance frequencies were out of the frequency range of the experiments, further analysis indicates that there was no obvious evidence of the effect of tank resonance on the wave loads of the lifeboat model for the tested wave frequencies. It was believed that there would be high damping for the free surface motions at these higher order resonance frequencies, and the resonance did not happen.

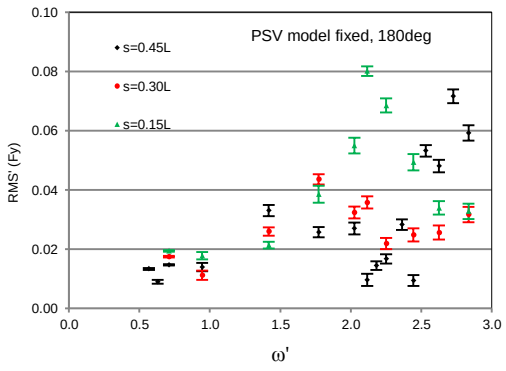

Fig. A1 Precision accuracy of non-dimensional sway force in head waves (PSV model fixed)

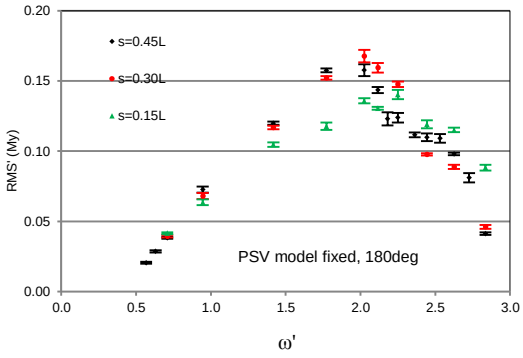

Fig. A2 Precision accuracy of the non-dimensional pitch moment in head waves (PSV model fixed)

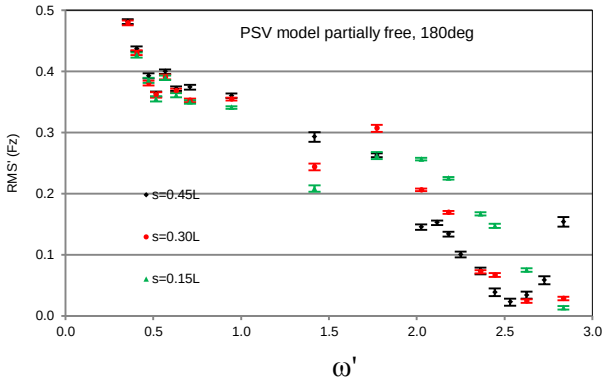

Fig. A3 Precision accuracy of the non-dimensional heave force in head waves (PSV model partially released)

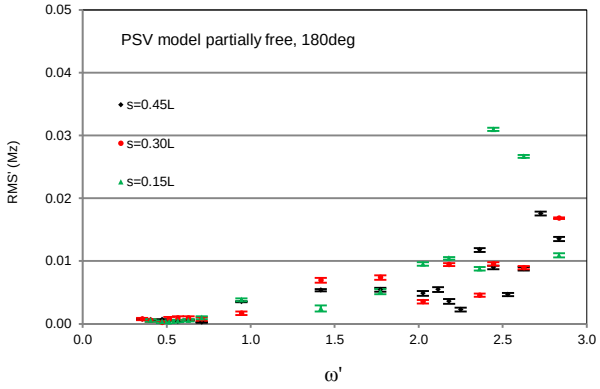

Fig. A4 Precision accuracy of the non-dimensional yaw moment in head waves (PSV model partially released)